Dimensional Control in Polyoxometalate Crystals Hybridized with Amphiphilic Polymerizable Ionic Liquids

Toshiyuki Misawa [1], Jun Kobayashi [1], Yoshiki Kiyota [1], Masayuki Watanabe [2], Seiji Ono [2], Yosuke Okamura [2], Shinichi Koguchi [1], Masashi Higuchi [2], Yu Nagase [2] and Takeru Ito [1,*]

[1] Department of Chemistry, School of Science, Tokai University, 4-1-1 Kitakaname, Hiratsuka 259-1292, Japan
[2] Department of Applied Chemistry, School of Engineering, Tokai University, 4-1-1 Kitakaname, Hiratsuka 259-1292, Japan
*   Correspondence: takeito@keyaki.cc.u-tokai.ac.jp; Tel.: +81-463-58-1211 (ext. 3737)

check for updates

Abstract: Ionic liquids are an important component for constructing functional materials, and polyxometalate cluster anion is a promising partner for building inorganic–organic hybrid materials comprising ionic liquids. In such hybrid materials, the precise control of the molecular arrangement in the bulk structures is crucial for the emergence of characteristic functions, which can be realized by introducing an amphiphilic moiety into the ionic liquids. Here, an amphiphilic polymerizable imidazolium ionic liquid with a methacryloyl group was firstly hybridized with polyoxometalate anions of octamolybdate ($[Mo_8O_{26}]^{4-}$, Mo_8) and silicotungstate ($[SiW_{12}O_{40}]^{4-}$, SiW_{12}) to obtain inorganic–organic hybrid crystals. The polymerizable ionic liquid with a octyl chain (denoted as $MAImC_8$) resulted in the formation of anisotropic molecular arrangements in the bulk crystal structure, which was compared with the hybrid crystals composed from the polymerizable ionic liquid without a long alkyl chain (denoted as MAIm). Rather densely packed isotropic molecular arrangements were observed in the hybrid crystals of $MAIm–Mo_8$ and $MAIm–SiW_{12}$ due to the lack of the amphiphilic moiety. On the other hand, using the amphiphilic $MAImC_8$ cation gave rise to a honeycomb-like structure with the Mo_8 anion and a layered structure with the SiW_{12} anion, respectively.

Keywords: inorganic–organic; hybrid crystal; ionic liquid; amphiphilic; polyoxometalate

1. Introduction

Ionic liquid molecules attract extensive attention from researchers owing to their characteristic properties such as conductivity, catalysis, and separation abilities [1–11]. These properties are quite attractive for the construction of functional materials. The hybridization of ionic liquids as organic components with other inorganic counter parts is effective for building up functional inorganic–organic hybrid materials. To select inorganic counter parts for the hybridization is crucial for improving the thermal stability and other properties.

Polyoxometalate (POM) cluster anions are effective inorganic components for constructing inorganic–organic hybrid materials due to their characteristic physicochemical properties [12–20]. Hybridization of ionic liquids with POMs has been investigated, and several functional hybrids have been successfully realized such as solid electrolytes or catalysts [21–28]. These ionic liquid–POM hybrids sometimes have POM arrangements in a disordered manner, which may be a drawback for exploiting their characteristics in solid-state hybrid materials. The dimensional control of the components in the solid state is quite significant for the emergence and control of characteristic properties [29]. Introducing amphiphilic moieties, such as a long alkyl chain [30–36] in ionic liquids

is an effective way of constructing single-crystalline ordered structures in the ionic liquid–POM hybrids [37–41].

Recently, we designed a polymerizable ionic liquid cation with an imidazolium moiety with a methacryloyl group ($[\{CH_2=C(CH_3)COO(CH_2)_2\}C_3H_3N_2(CH_3)]^+$, denoted as MAImC$_1$, Figure 1a), and successfully synthesized inorganic–organic hybrid monomers and polymers with several POM anions [42–44]. These MAImC$_1$–POM hybrids were isolated as single crystals with clarified structures, and behaved as monomers of hybrid polymers exhibiting high conductivity as solid electrolytes [44]. In the MAImC$_1$–POM hybrid monomers, the POM arrangements in the bulk crystal structures were isotropic due to the small molecular size of the MAImC$_1$ cation. Introducing an amphiphilic moiety into MAImC$_1$ will give rise to a more anisotropic molecular arrangement of POM anions derived from the structure-directing ability of the amphiphilic moiety [30–32].

Here we report the first syntheses of POM hybrid crystals with amphiphilic polymerizable ionic liquids. The amphiphilic polymerizable ionic liquid is a MAImC$_1$ derivative with a long octyl chain instead of a methyl group ($[\{CH_2=C(CH_3)COO(CH_2)_2\}C_3H_3N_2(C_8H_{17})]^+$, denoted as MAImC$_8$, Figure 1a). Another MAImC$_1$ derivative without a methyl group ($[\{CH_2=C(CH_3)COO(CH_2)_2\}C_3H_4N_2]^+$, denoted as MAIm, Figure 1a) was also utilized to hybridize with POM anions for comparison. The POM anions hybridized were β-type octamolybdate ($[Mo_8O_{26}]^{4-}$ (Mo$_8$), Figure 1b) and dodecatungstosilicate ($[SiW_{12}O_{40}]^{4-}$ (SiW$_{12}$), Figure 1b), both of which are anions with a 4− charge. Hybrid crystals with Mo$_8$ and SiW$_{12}$ have been reported previously [42,44]. The hybrid crystals with MAImC$_8$ contained anisotropic arrangements of POM anions in their bulk crystal structures due to the presence of an amphiphilic moiety, while hybrid crystals with MAIm exhibited isotropic POM arrangements.
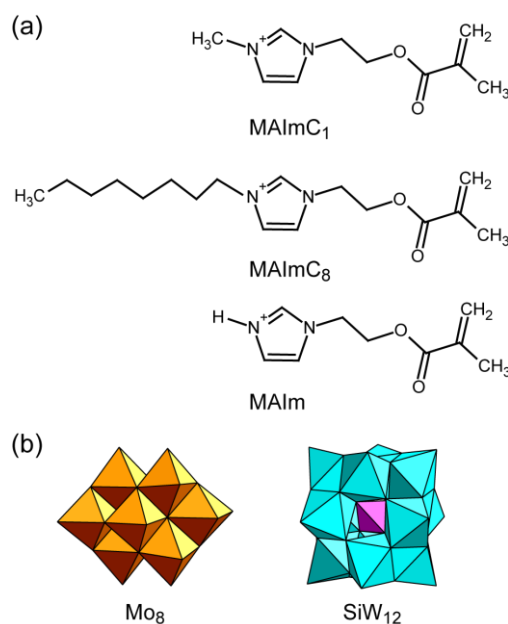
Figure 1. Molecular structures of the components: (**a**) polymerizable ionic liquids of MAImC$_1$, MAImC$_8$, and MAIm; (**b**) polyoxometalates of β-type octamolybdate (Mo$_8$) and dodecatungstosilicate (SiW$_{12}$) anions.

2. Materials and Methods

2.1. Materials and General Methods

All chemical reagents were purchased from FUJIFILM Wako Pure Chemical Corporation (Osaka, Japan) and Tokyo Chemical Industry Co., Ltd. (TCI, Tokyo, Japan). The starting polymerizable ionic liquid of $[\{CH_2=C(CH_3)COO(CH_2)_2\}C_3H_3N_2]$ (denoted as MAIm–N) was synthesized as a neutral

compound, and [{CH$_2$=C(CH$_3$)COO(CH$_2$)$_2$}C$_3$H$_3$N$_2$(C$_8$H$_{17}$)]Br (MAImC$_8$·Br) were synthesized as bromide salts according to previous studies (Figure S1) [42–44].

Infrared (IR) spectra were recorded on a Jasco FT/IR-4200ST spectrometer (JASCO Corporation, Tokyo, Japan) by the KBr pellet method. Powder X-ray diffraction (XRD) patterns were measured with a Rigaku MiniFlex300 diffractometer (Rigaku Corporation, Tokyo, Japan) by using Cu Kα radiation (λ = 1.54056 Å) at ambient temperature. CHN (carbon, hydrogen, and nitrogen) elemental analyses were performed with a PerkinElmer 2400II elemental analyzer (PerkinElmer, Waltham, MA, USA).

2.2. Syntheses of Polyoxometalate Hybrids with Polymerizable Ionic Liquids

2.2.1. Synthesis of MAIm–Mo$_8$

As-prepared MAIm–Mo$_8$ (denoted as **1**) was initially precipitated by a cation exchange reaction. Na$_2$MoO$_4$·2H$_2$O (1.0 g, 4.1 mmol) was dissolved in 10 mL of H$_2$O, and then the pH was adjusted to 3.8 by 6 M HCl. To the obtained homogeneous solution was added an ethanol solution (10 mL) of MAIm–N (0.28 g, 1.6 mmol) neutralized by 1 M HCl (2.0 mL). The resulting suspension was filtered to obtain colorless precipitates, which was dried under ambient atmosphere to obtain colorless precipitates (0.73 g, yield: 48%). An acetonitrile/ethanol solution (20 mL, 1:1 (*v/v*)) of as-prepared **1** (0.03 g) was heated at ca. 343 K for 3 h, and then the supernatant was slowly evaporated at room temperature to obtain colorless plates of **1**. CHN elemental analysis: Calcd for C$_{30}$H$_{45}$N$_6$NaMo$_8$O$_{32}$: C: 18.53, H: 2.25, N: 4.80%. Found: C: 18.97, H: 2.30, N: 4.98%. IR (KBr disk): 3144 (w), 3109 (w), 3010 (w), 2979 (w), 2927 (w), 2883 (w), 1734 (m), 1718 (m), 1635 (m), 1577 (w), 1543 (w), 1456 (w), 1401 (w), 1362 (w), 1317 (w), 1301 (m), 1170 (m), 1086 (w), 1041 (w), 942 (s), 916 (s), 846 (m), 817 (w), 724 (s), 666 (m), 626 (w), 556 (w), 523 (w) cm^{-1}.

2.2.2. Synthesis of MAImC$_8$–Mo$_8$

As-prepared MAImC$_8$–Mo$_8$ (denoted as **2**) was synthesized and recrystallized by a similar procedure to **1**. Na$_2$MoO$_4$·2H$_2$O (0.51 g, 2.1 mmol) dissolved in 10 mL of H$_2$O was adjusted to pH 3.8 by 6 M HCl, and then an ethanol solution (10 mL) of MAImC$_8$·Br (0.30 g, 0.80 mmol) was added. The resulting suspension was filtered and dried to obtain colorless precipitates (0.38 g, yield: 47%). An acetonitrile/ethanol solution (20 mL, 1:1 (*v/v*)) of as-prepared **2** (0.03 g) was heated at ca. 343 K for 3 hours, and the supernatant was slowly evaporated at room temperature to obtain colorless plates of **2**. CHN elemental analysis: Calcd for C$_{51}$H$_{87}$N$_6$NaMo$_8$O$_{32}$: C: 29.10, H: 4.26, N: 3.99%. Found: C: 28.05, H: 4.14, N: 3.52%. IR (KBr disk): 3136 (w), 3105 (w), 2956 (m), 2925 (s), 2854 (m), 1719 (m), 1636 (w), 1560 (w), 1457 (w), 1404 (w), 1377 (w), 1362 (w), 1317 (w), 1296 (w), 1162 (m), 1039 (w), 943 (s), 913 (s), 844 (m), 714 (s), 666 (m), 555 (w), 525 (w), 473 (w), 453 (w), 442 (w), 416 (w) cm^{-1}.

2.2.3. Synthesis of MAIm–SiW$_{12}$

As-prepared MAIm–SiW$_{12}$ (denoted as **3**) was synthesized by adding a 10 mL ethanol solution containing MAIm–N (0.59 g, 3.3 mmol) to a 10 mL ethanol solution of dodecatungstosilicic acid 26 hydrate (H$_4$[SiW$_{12}$O$_{40}$]·26H$_2$O (H–SiW$_{12}$), 2.0 g (0.60 mmol)). The obtained suspension was separated by decantation to obtain colorless precipitates, which were washed by water and dried under ambient atmosphere (1.3 g, yield: 51%). A 1,4-dioxane solution (20 mL) of as-prepared **3** (0.03 g) was heated at ca. 333 K for 3 h, and the supernatant was kept at 298 K to obtain colorless plates of **3**. CHN elemental analysis: Calcd for C$_{36}$H$_{52}$N$_8$SiW$_{12}$O$_{48}$: C: 12.01, H: 1.46, N: 3.11%. Found: C: 12.03, H: 1.47, N: 3.04%. IR (KBr disk): 3145 (w), 3072 (w), 2963 (w), 2927 (w), 1715 (m), 1634 (w), 1578 (w), 1547 (w), 1449 (w), 1404 (w), 1319 (w), 1297 (w), 1168 (m), 1085 (w), 1013 (w), 973 (s), 922 (s), 884 (w), 796 (s), 665 (w), 622 (w), 534 (w) cm^{-1}.

2.2.4. Synthesis of MAImC$_8$–SiW$_{12}$

As-prepared MAImC$_8$–SiW$_{12}$ (denoted as **4**) was synthesized and recrystallized by a similar procedure to **3**. H–SiW$_{12}$ (1.2 g, 0.36 mmol) was dissolved in 5 mL of ethanol, and then an ethanol solution (10 mL) of MAImC$_8$·Br (0.50 g, 1.3 mmol) was added. The resulting suspension was filtered and dried under ambient atmosphere to obtain colorless precipitates (1.2 g, yield: 69%). An 1,4-dioxane/ethanol solution (20 mL, 1:1 (*v/v*)) of as-prepared **4** (0.03 g) was heated at ca. 333 K for 3 hours, and the supernatant was kept at 298 K to obtain colorless plates of **4**. CHN elemental analysis: Calcd for C$_{68}$H$_{116}$N$_8$SiW$_{12}$O$_{48}$: C: 19.50, H: 2.79, N: 2.74%. Found: C: 20.18, H: 2.89, N: 2.77%. IR (KBr disk): 3142 (w), 3109 (w), 2957 (w), 2925 (m), 2853 (m), 1719 (w), 1635 (w), 1561 (w), 1457 (w), 1401 (w), 1377 (w), 1359 (w), 1318 (w), 1295 (w), 1161 (w), 1107 (w), 1054 (w), 1013 (w), 973 (m), 920 (s), 884 (w), 795 (s), 653 (w), 530 (w), 487 (w), 423 (w) cm^{-1}.

2.3. X-ray Crystallography

Single crystal X-ray diffraction measurements for **1**–**3** were performed with an ADSC Q210 CCD area detector by using synchrotron radiation (λ = 0.60000–0.80000 Å, Table 1) at 2D beamline in the Pohang Accelerator Laboratory (PAL, a synchrotron radiation facility in Pohang, Republic of Korea). The processing of both diffraction images and absorption correction were performed with HKL3000 [45]. The diffraction measurements for **4** were made on a Rigaku XtaLAB P200 diffractometer (Rigaku Corporation, Tokyo, Japan) using graphite monochromated Mo Kα radiation, and the data were collected and processed using CrysAlisPro [46]. The structures were solved by the dual-space algorithm using SHELXT Version 2014/5 [47] or SHELXS Version 2013/1 [48], and refined by the full-matrix least-squares method on F^2 using SHELXL Version 2014/7 [48]. All calculations were performed using the CrystalStructure software package [49]. Most non-hydrogen atoms were refined anisotropically, and the hydrogen atoms of organic moieties were refined using the riding model. Further details of the crystal structure investigation may be obtained free of charge from the Cambridge Crystallographic Data Centre, 12 Union Road, Cambridge CB2 1EZ, UK; fax: (+44) 1223 336 033; or E-Mail: deposit@ccdc.cam.ac.uk (CCDC 1934917–1934920).

3. Results

3.1. Mo$_8$ hybrids with Polymerizable Ionic Liquids

Octamolybdate (Mo$_8$) hybrids with the polymerizable ionic liquids of MAIm and MAImC$_8$ were obtained as colorless precipitates in ca. 50% yield. IR spectra of both as-prepared MAIm–Mo$_8$ (**1**, Figure 2a) and MAImC$_8$–Mo$_8$ (**2**, Figure 2c) exhibited characteristic peaks of the β-Mo$_8$ anion [50–52] in the range of 400–1000 cm^{-1} together with the peaks derived from MAIm or MAImC$_8$ (methylene groups in 2800–3000 cm^{-1} and methacryloyl group in 1200–1800 cm^{-1}), indicating the successful hybridization of Mo$_8$ with the polymerizable ionic liquids.

Both as-prepared precipitates of **1** and **2** were successfully recrystallized by using acetonitrile/ethanol solution to obtain single crystals. The IR spectra of recrystallized **1** (Figure 2b) were almost identical to that of the as-prepared **1** (Figure 2a), indicating that the molecular structures were retained before and after the recrystallization. The molecular structures of **2** were also the same before and after the recrystallization as observed in the IR spectra of hybrid crystal **2** (Figure 2c,d).

X-ray structure analyses together with CHN elemental analyses revealed that the Mo$_8$ hybrid crystals were formulated to be [{CH$_2$=C(CH$_3$)COO(CH$_2$)$_2$}C$_3$H$_4$N$_2$]$_3$Na[Mo$_8$O$_{26}$] for **1** and [{CH$_2$=C(CH$_3$)COO(CH$_2$)$_2$}C$_3$H$_3$N$_2$(C$_8$H$_{17}$)]$_3$Na[Mo$_8$O$_{26}$] for **2**, respectively (Table 1, Figure 3). Both hybrid crystals contained three MAIm (1+ charge) or MAImC$_8$ (1+ charge) and one Na$^+$ associated with one β-type Mo$_8$ anion (4− charge), being similar to other hybrid crystals consisting of β-type Mo$_8$ anions [42,53,54]. Both crystal structures contained a one-dimensional (1D) infinite chain composed of the Na$^+$ cation and Mo$_8$ anion (Mo$_8$–Na$^+$ 1D chain) as shown in Figure 3a,b, while the coordination environments of Na$^+$ were different. The Na$^+$ cation in **1** was surrounded by O atoms of two Mo$_8$
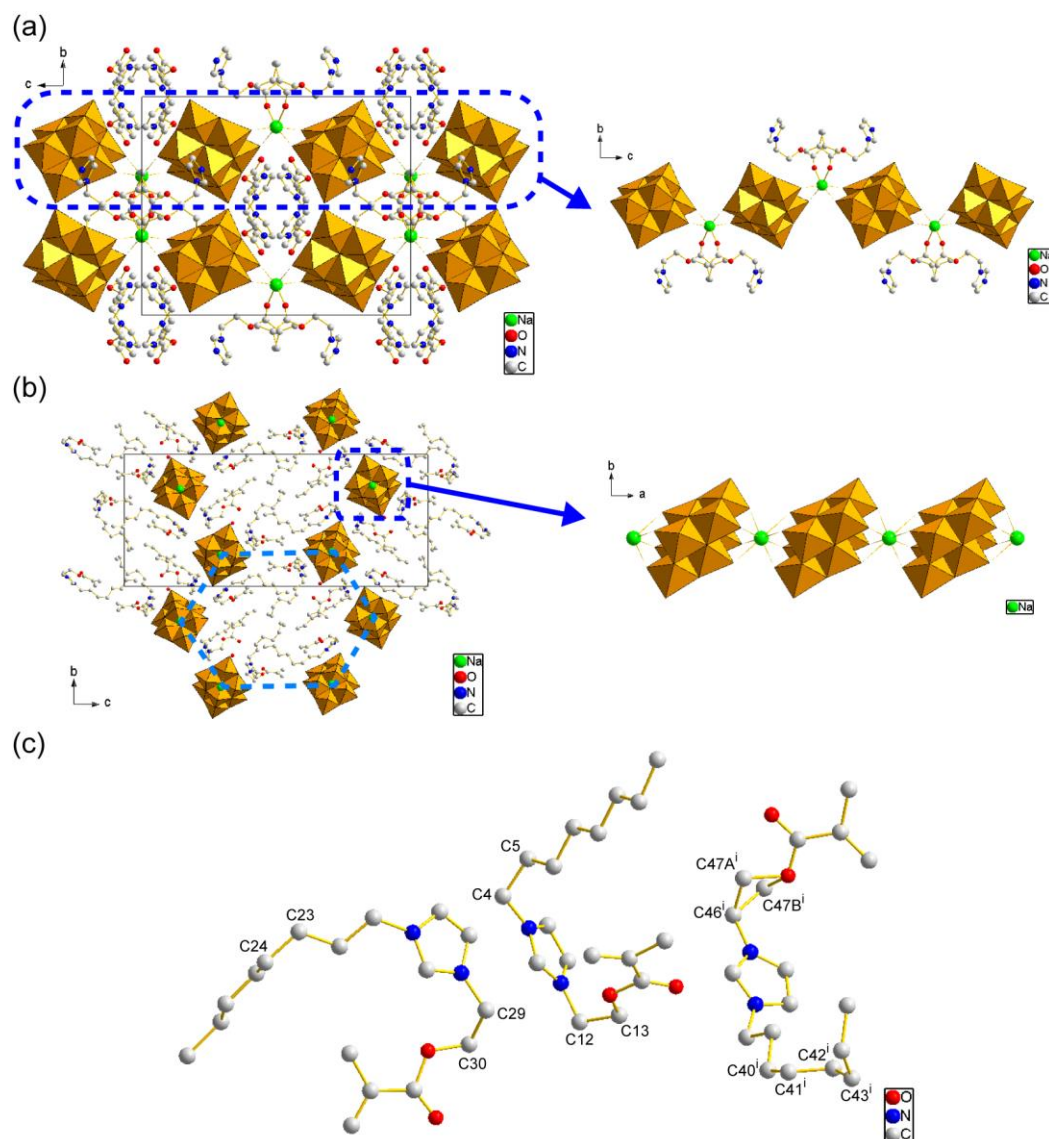
anions and two MAIm cations, and located in a six-fold coordination environment (Na–O distance: 2.28–2.43 Å, mean value: 2.36 Å) to form a zig-zag chain structure (Figure 3a, right). On the other hand, the Na^+ cation in **2** was sandwiched by only two β-Mo_8 anions to possess an eight-fold coordination environment (Na–O distance: 2.40–2.90 Å, mean value: 2.60 Å), resulting in a more straight chain structure (Figure 3b, right).
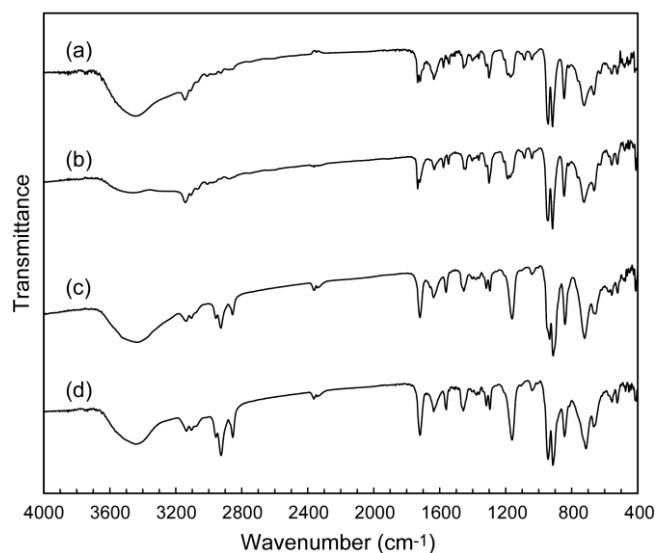
Figure 2. IR spectra of Mo_8 hybrid crystals: (**a**) as-prepared **1**; (**b**) recrystallized **1**; (**c**) as-prepared **2**; (**d**) recrystallized **2**.

Table 1. Crystallographic data of the hybrid crystals.

| Compound	1	2	3	4
Chemical formula	$C_{27}H_{39}N_6NaMo_8O_{32}$	$C_{51}H_{87}N_6NaMo_8O_{33}$	$C_{40}H_{60}N_8SiW_{12}O_{50}$	$C_{72}H_{107}N_8SiW_{12}O_{51}$
Formula weight	1750.14	2102.78	3687.22	4134.95
Crystal system	monoclinic	orthorhombic	monoclinic	monoclinic
Space group	*I2/a* (No. 15)	$P2_12_12_1$ (No. 19)	$P2_1/n$ (No. 14)	$P2_1/c$ (No. 14)
a (Å)	13.6080(3)	9.33330(10)	14.8460(3)	20.7451(16)
b (Å)	17.6620(4)	18.6205(2)	12.6020(3)	21.2737(6)
c (Å)	21.8453(5)	42.7175(5)	19.6940(5)	25.5199(8)
α (°)	90.0000	90.0000	90.0000	90.0000
β (°)	95.0422(14)	90.0000	98.6520(10)	103.067(5)
γ (°)	90.0000	90.0000	90.0000	90.0000
V ($Å^3$)	5230.1(2)	7423.90(14)	3642.61(15)	10970.9(10)
Z	4	4	2	4
ρ_{calcd} (g cm^{-3})	2.222	1.881	3.361	2.503
T (K)	100	100	100	100
Wavelength (Å)	0.80000	0.63000	0.60000	0.71075
μ (mm^{-1})	2.725	0.976	12.044	12.638
No. of reflections measured	35127	102284	94446	106869
No. of independent reflections	5143	15761	14513	24752
R_{int}	0.0600	0.0800	0.0870	0.1418
No. of parameters	394	883	507	644
R_1 ($I > 2\sigma(I)$)	0.0553	0.0564	0.0721	0.0777
wR_2 (all data)	0.1680	0.1576	0.2046	0.2256

Figure 3. Crystal structures of Mo$_8$ hybrid crystals (Na: green, C: gray, N: blue, O: red). Mo$_8$ anions are represented by polyhedrons. H atoms are omitted for clarity; (**a**) packing diagram of **1** (left, along *a* axis) and molecular arrangement of the Mo$_8$–Na$^+$ 1D chain in **1** (right, along *a* axis); (**b**) packing diagram of **2** (left, along *a* axis) and molecular arrangement of Mo$_8$-Na$^+$ 1D chains in **2** (right, along *c* axis). A honeycomb-like arrangement of Mo$_8$–Na$^+$ 1D chains is highlighted by a light-blue broken hexagon; (**c**) molecular conformations of crystallographically independent MAImC$_8$ cations in **2**. C atoms relevant to the *gauche* conformation are numbered. Symmetry code: (*i*) $1 - x$, $-0.5 + y$, $0.5 - z$.

In addition, the packing manners of the Mo$_8$–Na$^+$ 1D chains in the crystal structures of **1** and **2** were different. The Mo$_8$–Na$^+$ 1D chains in **1** were rather densely packed in the crystal structure (Figure 3a, left), while the Mo$_8$–Na$^+$ 1D chains in **2** were located more separately, to exhibit a honeycomb-like structure along the *a*-axis direction (Figure 3b, left). Namely, **1** had a rather isotropic arrangement of the Mo$_8$–Na$^+$ 1D chains, while **2** possessed a more anisotropic arrangement of the Mo$_8$–Na$^+$ 1D chains in the bulk crystal structure. This difference in the arrangements of the Mo$_8$–Na$^+$ 1D chains between **1** and **2** will be due to the presence of the amphiphilic moiety in the polymerizable ionic liquid cations. The MAImC$_8$ had a long alkyl chain, which interacted with itself to control the arrangement of the Mo$_8$–Na$^+$ 1D chain in the crystal structures of **2** [30–32]. As shown in Figure 3c, several C–C bonds in the methylene groups of MAImC$_8$ had a *gauche* conformation, which forced both octyl and methacryloyl groups to locate to the same side against the charged and hydrophilic imidazolium ring.

These molecular conformations of MAImC$_8$ caused the segregation of hydrophilic and hydrophobic parts in the crystal structure of **2**, resulting in the anisotropic honeycomb-like arrangement of the Mo$_8$–Na$^+$ 1D chains (Figure 3b, left). The octyl chains were not interdigitated in a straight manner.

　　　Powder XRD patterns of as-prepared **1** and **2** (Figure 4a,c) were quite similar in the peak positions to the patterns calculated from the single crystal structure of **1** and **2** (Figure 4b,d), indicating that the crystal structures of **1** and **2** were retained before and after the recrystallization. Slight differences in the peak intensity and position of the patterns may be derived from the difference in the measurement temperature (powder: ambient temperature, single crystal: 100 K). This suggests that the Mo$_8$–Na$^+$ 1D chains were already formed in the as-prepared precipitates due to their stable and rigid structures. The amphiphilic moiety of MAImC$_8$ in **2** also contributed to the formation of a stable and rigid crystal structure derived from the van der Waals interactions between the octyl chains.
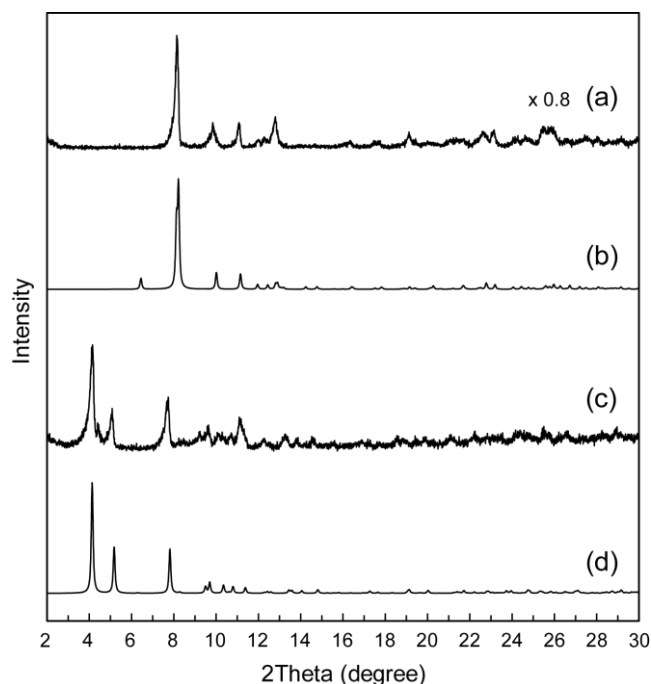
Figure 4. Powder XRD patterns of Mo$_8$ hybrid crystals: (**a**) as-prepared **1**; (**b**) calculated pattern of **1** using the structure obtained by single-crystal X-ray diffraction; (**c**) as-prepared **2**; (**d**) calculated pattern of **2** using the structure obtained by single-crystal X-ray diffraction.

3.2. SiW$_{12}$ Hybrids with Polymerizable Ionic Liquids

　　　Dodecatungstosilicate (SiW$_{12}$) hybrids with the polymerizable ionic liquids were obtained as colorless precipitates in ca. 50% yield for MAIm–SiW$_{12}$ (**3**) and ca. 70% yield for MAImC$_8$–SiW$_{12}$ (**4**), respectively. The characteristic peaks of SiW$_{12}$ [17,44,55] were observed for as-prepared **3** (Figure 5a) and **4** (Figure 5c) in the range of 400–1100 cm^{-1} of IR spectra. The presence of the polymerizable ionic liquids were confirmed by the IR spectra (in the range of 2800–3000 cm^{-1} for methylene groups and 1200–1800 cm^{-1} for methacryloyl group), which showed successful formation of the hybrid crystals comprising SiW$_{12}$ and the polymerizable ionic liquids.
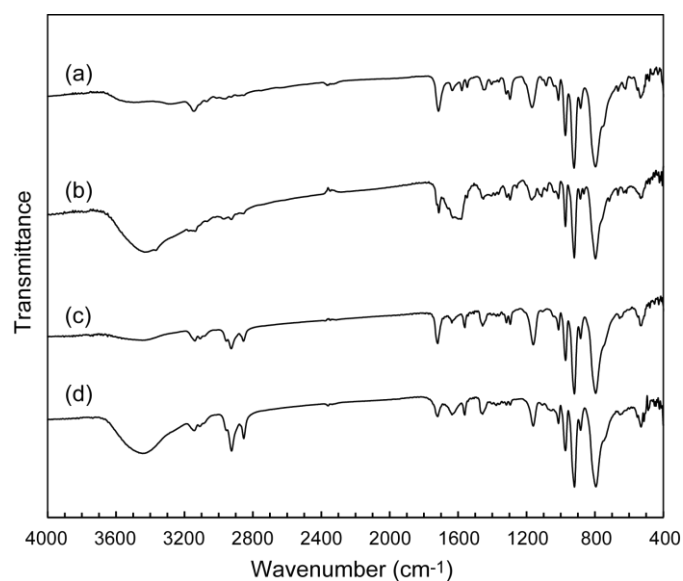
Figure 5. IR spectra of Mo_8 hybrid crystals: (**a**) as-prepared **3**; (**b**) recrystallized **3**; (**c**) as-prepared **4**; (**d**) recrystallized **4**.

Single crystals of **3** were obtained from 1,4-dioxane ($C_4H_4O_2$) solution, while single crystals of **4** were grown from 1,4-dioxane/ethanol solution. As-prepared **3** (Figure 5a) and recrystallized **3** (Figure 5b) were almost the same in the IR spectra, indicating the retention of the molecular structures before and after the recrystallization. A slight difference in the peaks in the range of 1500–1700 cm^{-1} may be derived from the difference in the crystal structures of as-prepared **3** and recrystallized **3** (see below). The retention of the molecular structures of **4** was also verified by the IR spectra measured before and after the recrystallization (Figure 5c,d).

Chemical formulae were revealed to be [{CH_2=C(CH_3)COO(CH_2)$_2$}$C_3H_4N_2$]$_4$[$SiW_{12}O_{40}$]·$C_4H_4O_2$ for **3** and [{CH_2=C(CH_3)COO(CH_2)$_2$}$C_3H_3N_2(C_8H_{17})$]$_4$[$SiW_{12}O_{40}$]·$C_4H_4O_2$·H_2O for **4**, respectively (Table 1). These hybrid crystals contained four polymerizable ionic liquid cations (1+ charge) associated with one SiW_{12} anion (4− charge). All of the protons of the starting H–SiW_{12} were replaced by ion-exchange reactions without remaining counter cations after the hybridization [44,56–58], which was different from the cases of Mo_8 hybrid crystals of **1** and **2**. Both recrystallized SiW_{12} hybrid crystals of **3** and **4** contained the solvents of crystallization (1,4-dioxane utilized in the recrystallization process for **3**; 1,4-dioxane and water for **4**), which also contrasts with the Mo_8 hybrid crystals of **1** and **2**. Figure 6 depicts crystal structures of **3** (Figure 6a) and **4** (Figure 6b). In both crystals, each SiW_{12} anion was isolated by the imidazolium moieties of the polymerizable ionic liquids (Figure 6a, right for **3**; Figure 6b, right for **4**).
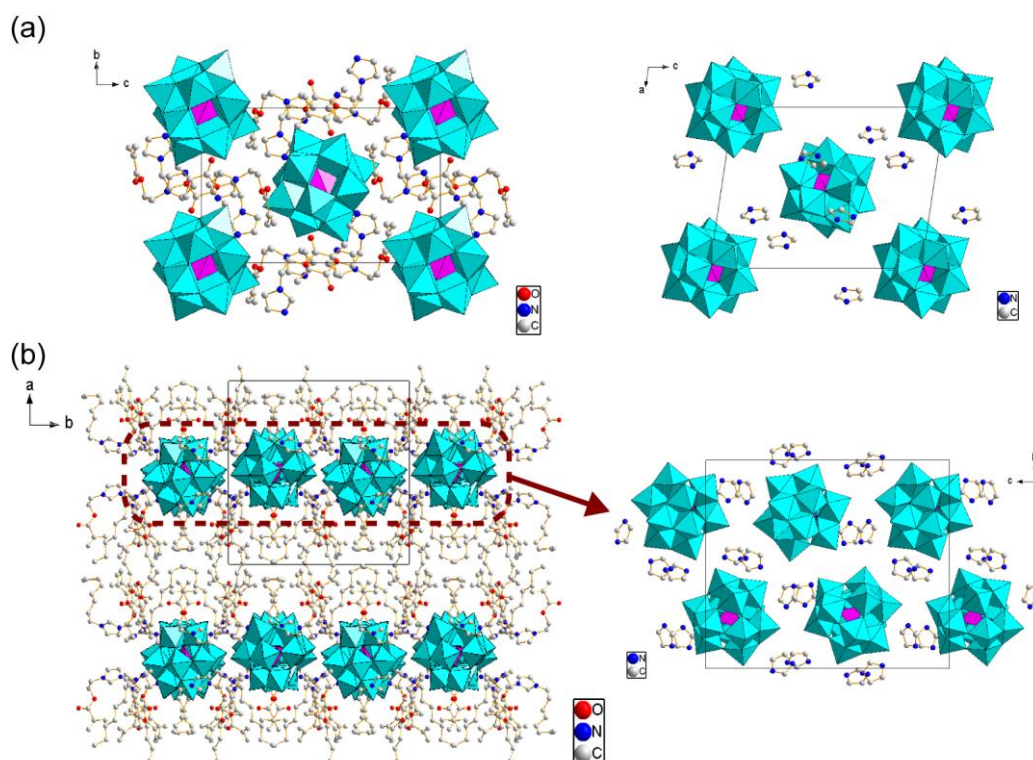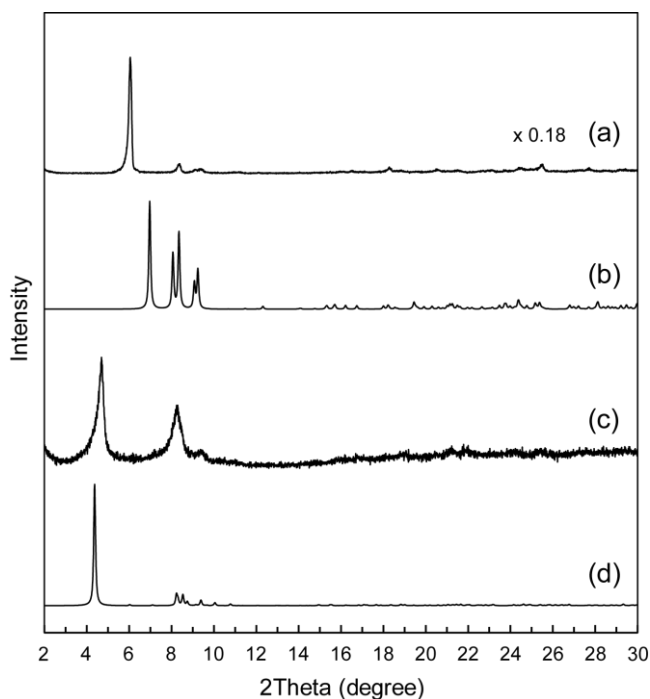
Figure 6. Crystal structures of SiW_{12} hybrid crystals (C: gray, N: blue, O: red). SiW_{12} anions are represented by polyhedrons. H atoms are omitted for clarity; (**a**) packing diagram of **3** (left, along *a* axis) and molecular arrangement of SiW_{12} anions in **3** (right, along *b* axis); (**b**) packing diagram of **4** (left, along *c* axis) and molecular arrangement of SiW_{12} anions in **4** (right, along *a* axis).

The molecular arrangements of the SiW_{12} anions in the bulk crystal structures of **3** and **4** were quite different. The SiW_{12} anions are arranged rather densely and isotropically in **3** (Figure 6a, left). On the contrary, the SiW_{12} anions in **4** formed the inorganic monolayers sandwiched by the $MAImC_8$ organic layers with an interlayer distance of 20.2 Å (Figure 6b, left), and exhibited much more anisotropic structure than **3**. Such anisotropic molecular arrangement will be induced by the amphiphilic moiety of the $MAImC_8$ cations. The $MAImC_8$ in **4** had similar conformations to those observed in **2** (Figure 3c). The octyl chains in **4** were not interdigitated in a straight manner as in the crystals of **2**.

The powder XRD pattern of as-prepared **3** (Figure 7a) was different from that calculated from the single crystal structure of **3** (Figure 7b). This demonstrates that the crystal structures of **3** changed after the recrystallization, probably because of desolvation of solvent molecules of the crystals under the ambient atmosphere. On the other hand, powder XRD patterns of as-prepared **4** (Figure 7c) were essentially similar to the patterns calculated from the single crystal structure of **4** (Figure 7d), indicating that the crystal structures of **4** were retained before and after the recrystallization. These results suggest that the amphiphilic moiety of the polymerizable ionic liquid enabled formation of the stable crystal structures of **4** owing to the van der Waals interactions between the octyl chains.

Figure 7. Powder XRD patterns of SiW$_{12}$ hybrid crystals: (**a**) as-prepared **3**; (**b**) calculated pattern of **3** using the structure obtained by single-crystal X-ray diffraction; (**c**) as-prepared **4**; (**d**) calculated pattern of **4** using the structure obtained by single-crystal X-ray diffraction.

4. Discussion

As observed in the crystal structures of **2** and **4**, introducing the amphiphilic moiety into the polymerizable ionic liquid enabled the construction of the anisotropic molecular arrangements of POM inorganic clusters in the bulk crystal structures. The amphiphilic MAImC$_8$ cation behaved as a structure-directing reagent, like typical surfactants [30–32], owing to the van der Waals interactions between the octyl chains of MAImC$_8$. The presence of a long alkyl chain in the polymerized ionic liquids induced the segregation of hydrophilic parts (charged POM and imidazolium ring) and a hydrophobic moiety (alkyl chain and methacryloyl group), which led to the formation of the anisotropic POM arrangements in the crystal structures of **2** and **4**. Introducing the amphiphilic moiety into the polymerizable ionic liquid also realized stable crystal structures. The crystal structures of **2** and **4** were retained before and after the recrystallization process, although the crystal structures of the hybrid crystal of **3** without the amphiphilic moiety changed in their crystal structures through the recrystallizations procedures.

The β-type Mo$_8$ anion tends to coordinate metal cations to form a 1D chain or two-dimensional (2D) layered structures [42,54]. The smaller metal cations such as Na$^+$ or Ag$^+$ preferred the 1D chain structure, while the larger cations such as K$^+$ or Cs$^+$ gave rise to a 2D layered structure. In the case of **1** and **2**, the Na$^+$ cation of the starting material (Na$_2$MoO$_4$·2H$_2$O) remained to form the Mo$_8$–Na$^+$ 1D chain structures in the crystal structures. Furthermore, **1** and **2** kept their molecular and crystal structures before and after the recrystallization (Figures 2 and 4), suggesting the retention of the Mo$_8$–Na$^+$ 1D chain structures. These stable Mo$_8$–Na$^+$ 1D chain structures could be beneficial to the Na$^+$-conducting materials. On the other hand, the typical Keggin-type SiW$_{12}$ anion exhibits T_d symmetry, which is higher than the C_{2h} symmetry of the β-Mo$_8$ anion (Figure 1b) [59,60]. The more spherical SiW$_{12}$ anion tends to be surrounded by the heterocyclic moiety of the polymerizable ionic liquid or surfactant [44,56], resulting in the isolated arrangement of SiW$_{12}$ without the coordination by metal cations.

As described here, introducing the amphiphilic moiety into the polymerizable ionic liquid is an effective way to control the POM arrangements in the hybrid single crystals. Such controlled arrangement of POM anions will have beneficial emergent functions such as conductive properties [12,13,29]. In principle, these POM hybrid crystals of **1**–**4** behave as inorganic–organic hybrid monomers to construct hybrid polymers [20,42–44], which could pave the way to another category of conductive materials. The polymerization of these hybrids and investigation of conductivities are in progress.

5. Patents

A Japanese patent (JP 2018012758 A) resulted from the work reported in this manuscript (T.I., Y.N., S.K., M.H., Y.O.).

References

1. Armand, M.; Endres, F.; MacFarlane, D.R.; Ohno, H.; Scrosati, B. Ionic liquid materials for the electrochemical challenges of the future. *Nat. Mater.* **2009**, *8*, 621–629. [CrossRef] [PubMed]

2. Kato, T.; Uchida, J.; Ichikawa, T.; Sakamoto, T. Functional liquid crystals towards the next generation of materials. *Angew. Chem. Int. Ed.* **2018**, *57*, 4355–4371. [CrossRef] [PubMed]

3. Welton, T. Room-temperature ionic liquids. Solvents for synthesis and catalysis. *Chem. Rev.* **1999**, *99*, 2071–2083. [CrossRef] [PubMed]

4. Wasserscheid, P.; Keim, W. Ionic liquids-new "solutions" for transition metal catalysis. *Angew. Chem. Int. Ed.* **2000**, *39*, 3772–3789. [CrossRef]

5. Mudring, A.-V.; Tang, S. Ionic liquids for lanthanide and actinide chemistry. *Eur. J. Inorg. Chem.* **2010**, *2010*, 2569–2581. [CrossRef]

6. Nishimura, N.; Ohno, H. 15th anniversary of polymerised ionic liquids. *Polymer* **2014**, *55*, 3289–3297. [CrossRef]

7. Watanabe, M.; Thomas, M.L.; Zhang, S.; Ueno, K.; Yasuda, T.; Dokko, K. Application of ionic liquids to energy storage and conversion materials and devices. *Chem. Rev.* **2017**, *117*, 7190–7239. [CrossRef]

8. Çelik, S.Ü.; Bozkurt, A.; Hosseini, S.S. Alternatives toward proton conductive anhydrous membranes for fuel cells: Heterocyclic protogenic solvents comprising polymer electrolytes. *Prog. Polym. Sci.* **2012**, *37*, 1265–1291. [CrossRef]

9. Kato, T.; Mizoshita, N.; Kishimoto, K. Functional liquid-crystalline assemblies: Self-organized soft materials. *Angew. Chem. Int. Ed.* **2006**, *45*, 38–68. [CrossRef]

10. Qian, W.; Texter, J.; Yan, F. Frontiers in poly(ionic liquid)s: Syntheses and applications. *Chem. Soc. Rev.* **2017**, *46*, 1124–1159. [CrossRef]

11. Nagase, Y.; Suleimenova, B.; Umeda, C.; Taira, K.; Oda, T.; Suzuki, S.; Okamura, Y.; Koguchi, S. Syntheses of aromatic polymers containing imidazolium moiety and the surface modification of a highly gas permeable membrane using the nanosheets. *Polymer* **2018**, *135*, 142–153. [CrossRef]

12. Coronado, E.; Gómez-García, C.J. Polyoxometalate-based molecular materials. *Chem. Rev.* **1998**, *98*, 273–296. [CrossRef] [PubMed]

13. Coronado, E.; Giménez-Saiz, C.; Gómez-García, C.J. Recent advances in polyoxometalate-containing molecular conductors. *Coord. Chem. Rev.* **2005**, *249*, 1776–1796. [CrossRef]

14. Long, D.-L.; Burkholder, E.; Cronin, L. Polyoxometalate clusters, nanostructures and materials: From self assembly to designer materials and devices. *Chem. Soc. Rev.* **2007**, *36*, 105–121. [CrossRef] [PubMed]

15. Nyman, M. Polyoxoniobate chemistry in the 21st century. *Dalton Trans.* **2011**, *40*, 8049–8058. [CrossRef]

16. Proust, A.; Matt, B.; Villanneau, R.; Guillemot, G.; Gouzerh, P.; Izzet, G. Functionalization and post-functionalization: A step towards polyoxometalate-based materials. *Chem. Soc. Rev.* **2012**, *41*, 7605–7622. [CrossRef] [PubMed]

17. Okuhara, T.; Mizuno, N.; Misono, M. Catalytic chemistry of heteropoly compounds. *Adv. Catal.* **1996**, *41*, 113–252.

18. Yamase, T. Photo- and electrochromism of polyoxometalates and related materials. *Chem. Rev.* **1998**, *98*, 307–325. [CrossRef] [PubMed]

19. Sadakane, M.; Steckhan, E. Electrochemical properties of polyoxometalates as electrocatalysts. *Chem. Rev.* **1998**, *98*, 219–237. [CrossRef] [PubMed]

20. Qi, W.; Wu, L. Polyoxometalate/polymer hybrid materials: Fabrication and properties. *Polym. Int.* **2009**, *58*, 1217–1225. [CrossRef]

21. Honma, I.; Yamada, M. Bio-inspired membranes for advanced polymer electrolyte fuel cells. Anhydrous proton-conducting membrane via molecular self-assembly. *Bull. Chem. Soc. Jpn.* **2007**, *80*, 2110–2123. [CrossRef]

22. Oh, S.-Y.; Yoshida, T.; Kawamura, G.; Muto, H.; Sakai, M.; Matsuda, A. Inorganic-organic composite electrolytes consisting of polybenzimidazole and Cs-substituted heteropoly acids and their application for medium temperature fuel cells. *J. Mater. Chem.* **2010**, *20*, 6359–6366. [CrossRef]

23. Wu, X.; Tong, X.; Wu, Q.; Ding, H.; Yan, W. Reversible phase transformation-type electrolyte based on layered shape polyoxometalate. *J. Mater. Chem. A* **2014**, *2*, 5780–5784. [CrossRef]

24. Bourlinos, A.B.; Raman, K.; Herrera, R.; Zhang, Q.; Archer, L.A.; Giannelis, E.P. A liquid derivative of 12-tungstophosphoric acid with unusually high conductivity. *J. Am. Chem. Soc.* **2004**, *126*, 15358–15359. [CrossRef]

25. Leng, Y.; Wang, J.; Zhu, D.; Ren, X.; Ge, H.; Shen, L. Heteropolyanion-based ionic liquids: Reaction-induced self-separation catalysts for esterification. *Angew. Chem. Int. Ed.* **2009**, *48*, 168–171. [CrossRef] [PubMed]

26. Rafiee, E.; Eavani, S. Polyoxometalate-based acid salts with tunable separation properties as recyclable Brönsted acid catalysts for the synthesis of β-keto enol ethers. *Catal. Commun.* **2012**, *25*, 64–68. [CrossRef]

27. Chen, X.; Souvanhthong, B.; Wang, H.; Zheng, H.; Wang, X.; Huo, M. Polyoxometalate-based ionic liquid as thermoregulated and environmentally friendly catalyst for starch oxidation. *Appl. Catal. B* **2013**, *138–139*, 161–166. [CrossRef]

28. Rickert, P.G.; Antonio, M.R.; Firestone, M.A.; Kubatko, K.-A.; Szreder, T.; James, F.; Wishart, J.F.; Dietz, M.L. Tetraalkylphosphonium polyoxometalate ionic liquids: Novel, organic-inorganic hybrid materials. *J. Phys. Chem. B* **2007**, *111*, 4685–4692. [CrossRef]

29. Kanatzidis, M.G. Discovery-Synthesis, Design, and prediction of chalcogenide phases. *Inorg. Chem.* **2017**, *56*, 3158–3173. [CrossRef]

30. Huo, Q.; Margolese, D.I.; Ciesla, U.; Demuth, D.G.; Feng, P.; Gier, T.E.; Sieger, P.; Firouzi, A.; Chmelka, B.F.; Schüth, F.; et al. Organization of organic molecules with inorganic molecular species into nanocomposite biphase arrays. *Chem. Mater.* **1994**, *6*, 1176–1191. [CrossRef]

31. Kanatzidis, M.G. Beyond silica: Nonoxidic mesostructured materials. *Adv. Mater.* **2007**, *19*, 1165–1181. [CrossRef]

32. Yamauchi, Y.; Kuroda, K. Rational design of mesoporous metals and related nanomaterials by a soft-template approach. *Chem. Asian J.* **2008**, *3*, 664–676. [CrossRef] [PubMed]

33. Song, Y.-F.; Long, D.-L.; Ritchie, C.; Cronin, L. Nanoscale polyoxometalate-based inorganic/organic hybrids. *Chem. Rec.* **2011**, *11*, 158–171. [CrossRef] [PubMed]

34. Yin, P.; Li, D.; Liu, T. Solution behaviors and self-assembly of polyoxometalates as models of macroions and amphiphilic polyoxometalate-organic hybrids as novel surfactants. *Chem. Soc. Rev.* **2012**, *41*, 7368–7383. [CrossRef] [PubMed]

35. Polarz, S.; Landsmann, S.; Klaiber, A. Hybrid surfactant systems with inorganic constituents. *Angew. Chem. Int. Ed.* **2014**, *53*, 946–954. [CrossRef] [PubMed]

36. Nisar, A.; Wang, X. Surfactant-encapsulated polyoxometalate building blocks: Controlled assembly and their catalytic properties. *Dalton Trans.* **2012**, *41*, 9832–9845. [CrossRef] [PubMed]

37. Ito, T. Inorganic–organic hybrid surfactant crystals: Structural aspects and functions. *Crystals* **2016**, *6*, 24. [CrossRef]

38. Kobayashi, J.; Kawahara, R.; Uchida, S.; Koguchi, S.; Ito, T. Conductive Hybrid Crystal Composed from Polyoxomolybdate and Deprotonatable Ionic liquid Surfactant. *Int. J. Mol. Sci.* **2016**, *17*, 994. [CrossRef]

39. Misawa, T.; Koguchi, S.; Niwa, K.; Kinoshita, Y.; Uchida, S.; Ito, T. Conductive hybrid crystal composed of polyoxovanadate and deprotonatable ionic liquid surfactant. *Inorg. Chem. Commun.* **2018**, *96*, 24–29. [CrossRef]

40. Jiang, Y.; Liu, S.; Li, S.; Miao, J.; Zhang, J.; Wu, L. Anisotropic ionic liquids built from nonmesogenic cation surfactants and Keggin-type polyoxoanions. *Chem. Commun.* **2011**, *47*, 10287–10289. [CrossRef]

41. Wang, K.; Zhuang, R. Ionic liquids of imidazolium salts comprising hexamolybdate cluster: Crystal structures and characterization. *Inorg. Chim. Acta* **2017**, *461*, 1–7. [CrossRef]

42. Kobayashi, J.; Misawa, T.; Umeda, C.; Isono, T.; Ono, S.; Naruke, H.; Okamura, Y.; Koguchi, S.; Higuchi, M.; Nagase, Y.; et al. Controlled introduction of metal cations into polymerizable ionic liquid-polyoxomolybdate hybrid crystals. *CrystEngComm* **2019**, *21*, 629–636. [CrossRef]

43. Ito, T.; Otobe, S.; Oda, T.; Kojima, T.; Ono, S.; Watanabe, M.; Kiyota, Y.; Misawa, T.; Koguchi, S.; Higuchi, M.; et al. Polymerizable ionic liquid crystals comprising polyoxometalate clusters toward inorganic-organic hybrid solid electrolytes. *Polymers* **2017**, *9*, 290. [CrossRef] [PubMed]

44. Ito, T.; Kiyota, Y.; Oda, T.; Watanabe, M.; Ono, S.; Oda, Y.; Misawa, T.; Isono, T.; Otobe, S.; Okamura, Y.; et al. Highly conductive polymer electrolytes constructed from polymerizable ionic liquid and inorganic cluster. *Trans. Mater. Res. Soc. Jpn.* **2019**, *44*, 101–107. [CrossRef]

45. Otwinowski, Z.; Minor, W. Processing of X-ray diffraction data collected in oscillation mode. *Methods Enzymol.* **1997**, *276*, 307–326. [PubMed]

46. *CrysAlisPro ver. 1.171.39.46*; Rigaku Corporation: Oxford, UK, 2016.

47. Sheldrick, G.M. SHELXT—Integrated space-group and crystal structure determination. *Acta Crystallogr. Sect. A* **2015**, *71*, 3–8. [CrossRef] [PubMed]

48. Sheldrick, G.M. A short history of SHELX. *Acta Crystallogr. Sect. A* **2008**, *64*, 112–122. [CrossRef] [PubMed]

49. *CrystalStructure 4.3*; Rigaku Corporation: Tokyo, Japan, 2019.

50. Klemperer, W.G.; Shum, W. Synthesis and interconversion of the isomeric α- and β-$Mo_8O_{26}{}^{4-}$ ions. *J. Am. Chem. Soc.* **1976**, *98*, 8291–8293. [CrossRef]

51. Himeno, S.; Niiya, H.; Ueda, T. Raman studies on the identification of isopolymolybdates in aqueous solution. *Bull. Chem. Soc. Jpn.* **1997**, *70*, 631–637. [CrossRef]

52. Cruywagen, J.J. Protonation, oligomerization, and condensation reactions of vanadate(V), molybdate(VI), and tungstate(VI). *Adv. Inorg. Chem.* **1999**, *49*, 127–182.

53. Ito, T.; Mikurube, K.; Abe, Y.; Koroki, T.; Saito, M.; Iijima, J.; Naruke, H.; Ozeki, T. Hybrid inorganic-organic crystals composed of octamolybdate isomers and pyridinium surfactant. *Chem. Lett.* **2010**, *39*, 1323–1325. [CrossRef]

54. Mikurube, K.; Hasegawa, K.; Matsumoto, T.; Kobayashi, J.; Naruke, H.; Ito, T. Isomerization-induced introduction of metal cations into polyoxomolybdate-surfactant hybrid crystals. *Inorg. Chem. Commun.* **2016**, *73*, 45–48. [CrossRef]

55. Rocchiccioli-Deltcheff, C.; Fournier, M.; Franck, R.; Thouvenot, R. Vibrational investigations of polyoxometalates. 2. Evidence for anion-anion interactions in molybdenum(v1) and tungsten(v1) compounds related to the Keggin structure. *Inorg. Chem.* **1983**, *22*, 207–216. [CrossRef]

56. Otobe, S.; Kiyota, Y.; Magira, S.; Misawa, T.; Fujio, K.; Naruke, H.; Uchida, S.; Ito, T. Conductive inorganic–organic hybrid layered crystals composed of Keggin-type polyoxotungstates and a heterocyclic surfactant. *Eur. J. Inorg. Chem.* **2019**, *2019*, 442–447. [CrossRef]

57. Nyman, M.; Ingersoll, D.; Singh, S.; Bonhomme, F.; Alam, T.M.; Brinker, C.J.; Rodriguez, M.A. Comparative study of inorganic cluster-surfactant arrays. *Chem. Mater.* **2005**, *17*, 2885–2895. [CrossRef]

58. Nyman, M.; Rodriguez, M.A.; Anderson, T.M.; Ingersoll, D. Two structures toward understanding evolution from surfactant-polyoxometalate lamellae to surfactant-encapsulated polyoxometalates. *Cryst. Growth Des.* **2009**, *9*, 3590–3597. [CrossRef]

59. Bridgeman, A.J.; Cavigliasso, G. Electronic structure of the α and β isomers of $[Mo_8O_{26}]^{4-}$. *Inorg. Chem.* **2002**, *41*, 3500–3507. [CrossRef] [PubMed]

60. Bridgeman, A.J.; Cavigliasso, G. A comparative investigation of structure and bonding in Mo and W $[TeM_6O_{24}]^{6-}$ and $[PM_{12}O_{40}]^{3-}$ heteropolyanions. *J. Phys. Chem. A* **2003**, *107*, 6613–6621. [CrossRef]